Journal of Materials Processing Tech. 250 (2017) 379–389

Contents lists available at ScienceDirect

Journal of Materials Processing Tech.

journal homepage: www.elsevier.com/locate/jmatprotec

Improving energy efficiency in friction assisted joining of metals and polymers

Francesco Lambiase[a,b,*], Alfonso Paoletti[a,b], Valentino Grossi[a], Silvio Genna[b,c]

[a] Department of Industrial and Information Engineering and Economics, University of L'Aquila, via G. Gronchi 18, Zona Industriale di Pile, 67100 (AQ), Italy
[b] CIRTIBS Research Centre, University of Naples Federico II, P. le Tecchio 80, 80125 Naples (NA), Italy
[c] Department of Enterprise Engineering, University of Rome Tor Vergata, Via del Politecnico 1, 00133 Rome, Italy

ARTICLE INFO

Keywords:
Friction assisted joining
Direct-joining
Joining
Process efficiency
Laser texturing
Thermal analysis
Energy analysis

ABSTRACT

The influence of the clamping frame material in Friction Assisted Joining of polymer-metal sheets is investigated. An experimental campaign was conducted by varying the clamping frame material (steel and wood) and the heating time. The process was applied to join Al-Mg aluminum alloy and Polyvinyl Chloride sheets. Thermal analysis and energy measurements were conducted during the process. The morphology, fracture surface and strength of the joints were analyzed. The clamping frame made of wood enabled different advantages to be achieved, including reduction of the energy loss towards the clamping frame, faster heating of the materials being joined, and more uniform distribution of the temperature over the joining area, which resulted in increased mechanical strength. Under optimal conditions the joint efficiency approached 97%.

1. Introduction

The increasing employment of multi-materials hybrid structures is attracting growing attention in different production fields including automotive, aerospace, biomedical, civil constructions etc. Among the main issues introduced by such structures, the coupling of different materials often involves many difficulties owing to the great chemical, mechanical, physical and thermal differences of such materials. Common joining processes (adhesive bonding and mechanical joining) involve several limitations and problems. The mechanical joining process generally requires pre-drilled holes for the insertion of an external fastener, which increases the structure weight and joining costs. A number of processes have been introduced to overcome this problem including fast joining processes: Self Pierce Riveting (SPR), and Mechanical Clinching (MC). Di Franco et al. (2012) demonstrated the feasibility of using SPR to join aluminum sheet with thin CFRP laminates and discovered that the process enabled a great reduction in the processing time because the predrilled hole was not required. Similarly, MC was extended to join metals with composite materials achieving the additional advantage of the absence of expensive external fasteners. Lambiase and Ko (2016) investigated direct clinching (without performing the pre-drilled hole) and found that, despite the great material plastic deformation of the aluminum sheet during the mechanical clinching of the aluminum and CFRP sheets, the damaged region of the laminate was relatively confined, since a great part of the damaged CFRP was ejected from the joint. Lambiase and Ko (2017) also showed that the adoption of a reshaping step can increase the strength of clinched joints made on aluminum and CFRP sheets by almost 30%. This was due to an increase in both the neck thickness and the undercut. Lee et al. (2014) investigated the hole-clinching process to reduce the delamination in the CFRP. The authors found that the CFRP damage was almost completely avoided; however, the process was characterized by concentricity issues between the punch and the hole and a longer processing time, because of the hole drilling. Lambiase and Durante (2017) investigated the suitability of hole punching of composite materials to reduce the hole manufacturing time. This study demonstrated that hole punching of GFRP sheets can dramatically cut the processing time with a limited delamination near the hole. Thus, it could be used for producing holes in composite materials that are addressed to subsequent clinching.

In general, when dealing with the mechanical joining two main issues have to be faced: the process time to produce the holes in the sheets (even though even on composite material this time can be dramatically reduced) and stress concentration around the joints, which affects the mechanical behavior of the structure. On the other hand, adhesive bonding produces more uniform distribution of stress over the joining area but it comes with a series of requirements including accurate cleaning of the substrates by means of mechanical machining or even chemical agents (generally solvents), a long curing time, high sensitivity to the adhesive thickness, environment (e.g. moisture), and

* Corresponding author at: Department of Industrial and Information Engineering and Economics, University of L'Aquila, via G. Gronchi 18, Zona Industriale di Pile, 67100 (AQ), Italy.
E-mail address: francesco.lambiase@univaq.it (F. Lambiase).

http://dx.doi.org/10.1016/j.jmatprotec.2017.08.005
Received 28 May 2017; Received in revised form 29 July 2017; Accepted 3 August 2017
Available online 05 August 2017
0924-0136/ © 2017 Elsevier B.V. All rights reserved.

temperature. In addition, the mechanical behavior of adhesive bonds shows a great long term uncertainty.

In order to overcome such limitations, several processes have recently been developed to produce hybrid structures involving different materials such as metals and polymers or composite laminates, including Friction Stir Welding, Laser-Assisted Joining (LAJ), Friction Assisted Joining (FAJ), friction riveting, friction based stacking, etc. Khodabakhshi et al. (2017) proved the suitability of FSW to join aluminum and High Density Polyethylene sheets by means of Friction Stir Welding. The process enabled butt joints to be produced. Abibe et al. (2016) investigated Friction Based Stacking to join aluminum Al-Mg-Si alloy with polyetherimide in an overlap configuration. The process consisted in thermoforming of a thermoplastic polymer by means of a rotating tool to produce an undercut with a predrilled hole made on the metal part. Laser Assisted Joining and Friction Assisted Joining are also very promising joining processes for direct joining of metals and plastics. Actually, they involve localized heating of a thin layer of material, which leads to a high energy efficiency, while they require relatively low clamping forces and produce joints with high strengths.

Katayama and Kawahito (2008) investigated the mechanisms that fasten the sheets after Laser Assisted Joining. The authors found that, the joint is made by both physical/chemical bonding between the substrates and the penetration of the polymer in the metal roughness. In both these processes, the polymer is heated and softened, thus, the simultaneous action of the clamping pressure and high temperature enables the formation of the joint. Thus, the quality of these joints strongly depends on the thermal history and spatial distribution of temperature. To this end, Lambiase and Genna (2017) applied the LAJ process to join AISI304 and polycarbonate and determined the main processing window (temperature of joining “activation”, development of tunnel defect etc.). Lambiase et al. (2017) also demonstrated the suitability of the LAJ process for joining composite materials with thermoplastic polymers. The authors discovered that the process consisted in the substitution of the covering (thermosetting) epoxy matrix with the thermoplastic polymer.

FAJ is relatively similar to LAJ with the difference that the materials are heated by means of frictional work instead of a laser source. Liu et al. (2014) studied the influence of the process parameters (interaction time and tool rotational speed) on the thickness of the melted polymer during Friction Lap Welding of Al-Mg-Si alloy with polyamide. Goushegir et al. (2015) studied the influence of the heating time, tool rotation speed, and plunging speed on the strength of the joints made by Al-Cu/carbon-fiber-reinforced poly(phenylene sulfide) by means of friction spot joints. Yusof et al. (2016) investigated the effects of the surface states and process parameters on defects produced by means of the Friction Spot Joining process on Al-Mg alloy sheets with Polyethylene Terephthalate. When joining by means of the LAJ or FAJ processes, the temperature strongly influences the quality of the joints since it influences the energy of joint “activation”, polymer viscosity as well as polymer degradation. For this reason, Goushegir et al. (2014) studied the influence of temperature on microstructure and mechanical performance during Friction Spot Joining. However, also the surface conditions of the sheets play a crucial role in the quality and strength of such joints.

Yusof et al. (2012) proved that the anodizing pretreatment of aluminum sheets can significantly increase the strength of the joints made by LAJ. Okada et al. (2014) found similar results while joining Al-Cu alloy with Polyethylene sheet by Friction Lap Welding. Aluminum anodization promoted intermolecular force and Coulomb’s force to arise between the carbonyl group and oxide film on aluminum alloy and then the materials were joined in addition to an anchor effect.

The strength of the joints is also influenced by the surface roughness of the metal part. Nagatsuka et al. (2015) proved that surface grinding provided beneficial effects on the mechanical strength of Friction Lap Joints made on Al-Mg alloy with carbon-fiber–reinforced plastic. Zhang et al. (2016) further stressed the concept of surface modification to improve the strength of this type of joints. The authors, performed laser texturing on aluminum substrates in order to produce micro-mechanical interlocks between aluminum and CFRP sheets during LAJ. Rodríguez-Vidal et al. (2016) optimized laser textures to optimize the strength of T-joints performed on polymer metal plates by means of LAJ. Pardal et al. (2017) showed the advantages of laser texturing to improve the strength of metal to metal joints performed by LAJ.

When dealing with Laser Assisted Joining as well as Friction Assisted Joining, the strength of the joint is greatly influenced by the temperature field produced, which in turn depends on the thermal characteristics of the materials involved and process parameters. The temperature history but also its spatial distribution also depend on the material of the clamping frame. However, no study has been conducted to evaluate how the heat conduction towards the clamping fame influences the joining process and the quality of the joints.

In the present investigation, thin sheets made of AA5053 aluminum alloy were joined to polyvinyl chloride (PVC) sheets by means of the Friction Assisted Joining process. These materials were selected due to their extensive combined employment (e.g. window fixtures, etc.). Two materials were adopted for the clamping frame: wood and steel (C40). These materials were selected because of the great difference in their thermal conductivity (C40 steel has a thermal conductivity almost 250 times greater than that of wood). The heating time was also varied. Thus, a comparative study of the process was conducted by measuring: the temperature distribution and evolution during the process, the torque and the energy absorbed. In addition, to assess the quality of the joints mechanical characterization tests, morphological analysis and fracture surface analysis were performed.

2. Materials and methods

2.1. Specimens preparation

Rolled sheets with 2 mm thickness of AA5053 aluminum alloy were joined to polyvinyl chloride (PVC) with 4 mm thickness. Mechanical characterization of the base material was performed by conducting tensile tests according to ASTM E (2000b) E08 (2000b) and ASTM D (2000a) D638 (2000a) (Type 4) standards for the aluminum and PVC, respectively. Thermogravimetric tests were conducted to investigate the decomposition temperature of the PVC and wood (of the clamping frame) materials by means of a machine model L81/1550 by LINSEIS. The tests were conducted at the highest heating rate allowed by the machine 40 °C/min. The main mechanical and thermal properties of the materials are summarized in Table 1.

Before joining, both the materials were cleaned by means of an ultrasonic bath (water and ethanol) to degrease the sheets (for an

Table 1
Main mechanical properties of the materials.

Material	Young Modulus [GPa]	Yield Strength $\sigma_{y0.2}$ [MPa]	Tensile Strength, σ_{max}[MPa]	Elongation at rupture [%]	Melting Temperature [°C]	Thermal Conductivity [W m^{-1} K^{-1}]	Decomposition Temperature [°C]
AA5053	67	100	250	15	607–649 °C	138	
PVC	2.8		37	2	> 210 Yu et al. (2016)	0.19	293

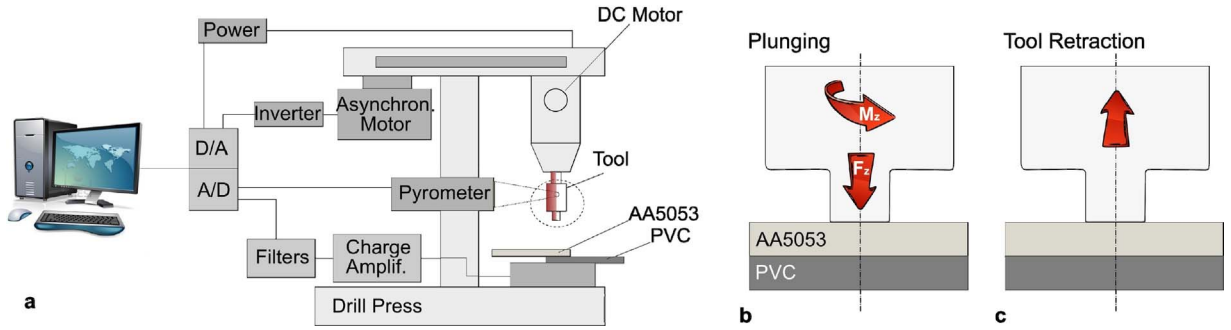

Fig. 1. (a) Schematic representation of the adopted CNC instrumented machine, (b) plunging and (c) retraction phases.

Table 2
Main Thermal characteristics of materials used for clamping frames.

Materials	Thermal conductivity [W m^{-1} K^{-1}]	Characteristic temperatures
C40 (Steel)	25	> 1450 °C-Melting
Walnut wood	0.04 Matweb (2016)	260 °C-onset of degradation from TGA

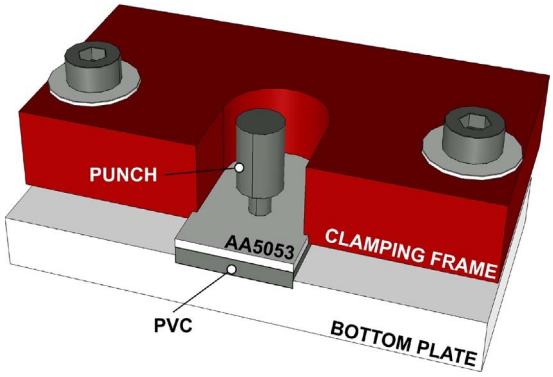

Fig. 2. Schematic representation of the adopted setup.

immersion time of 10 min). To improve the mechanical strength of the joints (due to the poor chemical affinity of the two materials) laser texturing was employed. To this end, the surface of the aluminum specimens was treated by means of laser ablation to produce a textured structure. A 30 W fiber laser (YLP-RA30-1-50-20-20 by IPG) was adopted for this purpose. A square-net path was used with the following processing conditions: average power 30 W, pulse frequency 30 kHz, scanning speed 1000 mm/s, hatch distance (i.e. the distance between two consecutive lines) 0.3 mm, and 20 repetitions for each path.

2.2. Joining procedure

The joints were produced by applying a constant controlled plunging force during the FAJ process. To this end, an instrumented CNC machine equipped with a two-component (F_z–plunging force, M_z–torque) piezo-electric cell by Kistler, and a position transducer were used in the experiments. A schematic representation of the adopted CNC machine is reported in Fig. 1a.

The process consisted of two phases: first the tool rotates at a given speed (ϖ = 5400 rpm) and plunged with a constant plunging force (F_j = 320 N) for a prescribed heating time D_t, as schematically reported in Fig. 1b. During the first phase, the aluminum sheet, which is placed at the punch side, is heated up due to the frictional heat developing at the tool-sheet interface. The heat absorbed is rapidly conducted towards the PVC material, which softens and adheres to the aluminum bottom surface. However, part of the heat absorbed by the aluminum is conducted towards the clamping frame that is used to ensure a stable contact between the materials without relative motions during both the process phases. Then, the tool is retracted to allow the materials to cool down, as reported in Fig. 1c.

An experimental campaign was conducted by varying the material of the clamping frame and the heating time (between 5 s and 30s). The maximum value of the heating time was chosen to avoid excessive thinning and degradation of the polymer. To this end, some preliminary tests with a longer heating time were conducted. Five replicates were performed for each joining condition and the main statistical parameters, including mean and standard deviation were performed.

A cylindrical tool with an end tip diameter of 5 mm made of hardened K340 high strength steel was used in all the tests. On the other hand, two clamping frames with the same geometry and different materials (low carbon steel C40 and walnut wood) were utilized. The main thermal characteristics of the materials used for the clamping frames are reported in Table 2.

A schematic representation of the adopted setup is reported in Fig. 2.

The energy input (Q) for the different processing conditions was calculated by means of torque measurements during the joining process, by means of Eq. (1), whereas the rotation speed ω [rad/s] is constant throughout the process.

$$Q = \int M_z \cdot \omega dt = \omega \int M_z dt \qquad \text{Eq. (1)}$$

Infrared thermography (infrared camera model E60 by FLIR) was used to monitor the process temperature of both the specimen and the clamping frame with an acquisition rate of 30 Hz. The camera was placed at an angle of 60 ° with respect to the aluminum sheet at a distance of 320 mm. In addition, given the low emissivity of the

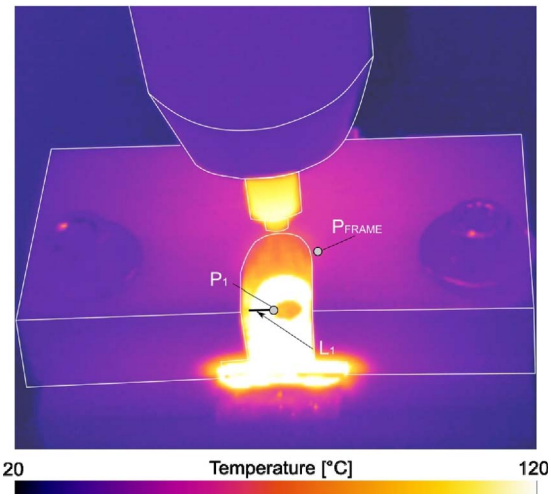

Fig. 3. Schematic representation of main measurement tools used for infrared thermography.

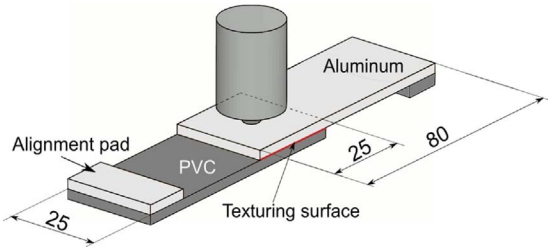

Fig. 4. Schematic representation of the specimen used in single lap shear tests.

aluminum surface and to homogenize the clamping frame emissivity, the surfaces were covered by means of a thin layer of graphite. Different measurements were performed in order to better investigate the difference of temperature achieved with the two types of clamping frame, including the temperature history on points P_{FRAME} (top surface of clamping frame) and P_1 (temperature of aluminum near tool edge) and the temperature distribution on lines L_1 (radial variation on top surface of aluminum), as schematized in Fig. 3.

The mechanical behavior of the joints was assessed by means of Single Lap Shear Tests (SLST). A schematic of the specimen is reported in Fig. 4. SLST were performed under a constant cross-head speed of 2 mm/min by means of a testing machine model 322.121 by MTS equipped with a load cell with 25 kN full scale. The strength of the joints τ_r was evaluated by dividing the maximum load measured in the test by the joined area (measured after each test).

The features of the joints were assessed by means of cross sections as well as fracture surfaces after the mechanical tests. The joints were cut near the middle cross section by means of an abrasive cutting blade and prepared according to standard procedures for metallographic specimen preparation.

The morphology of the fractured surfaces was also observed by means of Scanning Electron Microscopy (SEM) and a digital microscope (KH-8700 by Hirox) equipped with a 2.11 mega-pixel CCD sensor. A MXG5040RZ lens was adopted using a relatively low magnification (50 × –400 ×) and the tiling tool was used to acquire the image of the entire joined area.

3. Results and discussion

3.1. Mechanism of friction assisted joining

Fig. 5 shows the 3D view (in true and pseudo color) of the texture produced on the aluminum sheets. As can be inferred, the surface texture, produced by laser ablation produces both grooves and teeth, which are due to material reflow during interaction of the laser beam with the material. Under the adopted processing conditions, the groove depth and teeth height were in the range 65–70 μm. During Friction Assisted Joining, the aluminum teeth penetrate the underlying polymer, which rapidly softens and reflows towards the aluminum grooves. Thus, a series of micromechanical interlocks are produced that fasten the substrates.

The quality of the joints depends on the temperature produced at the sheets interface and the contact pressure. Thus, because of the small dimensions of the pin (as compared to the specimen surface), temperature gradients are produced leading to different joining conditions between the material under the tool and that in more external regions. Optimal joining conditions would lead to the achievement of a uniform optimal temperature distribution over the joining area, which enables enough polymer softening to produce a good material flow (without producing thermal degradation of the polymer).

However, a thermal gradient exists between the material under the tool pin and in the more peripheral regions that causes different joining conditions in the same specimen, as depicted in Fig. 6.

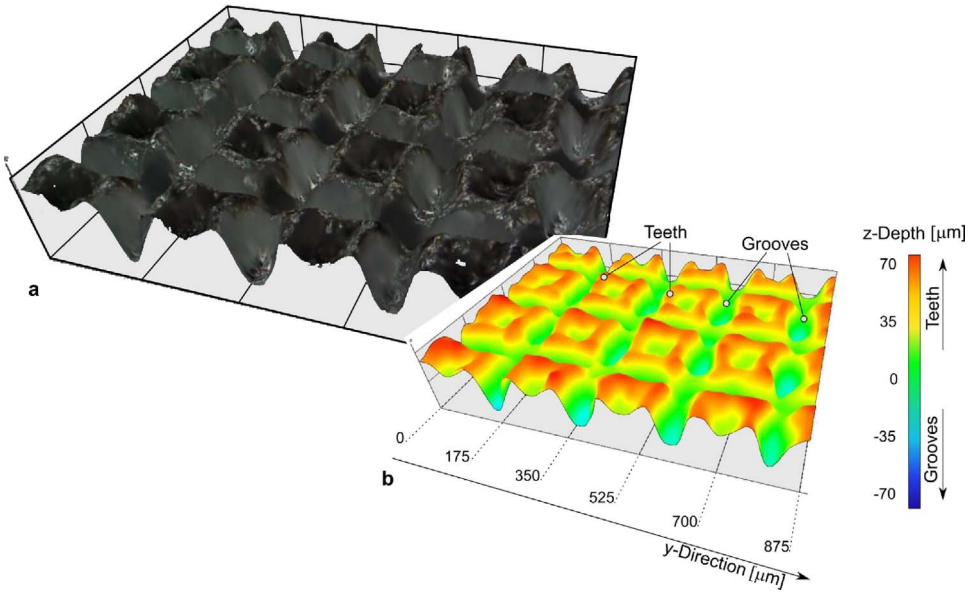

Fig. 5. 3D view of the texture produced on aluminum sheet.

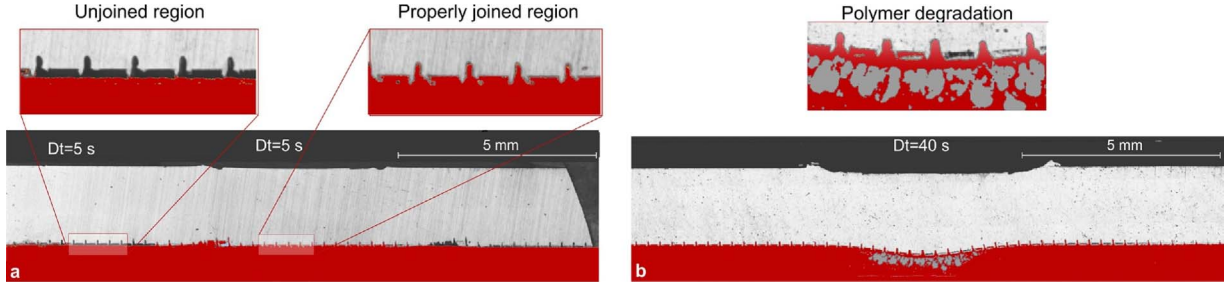

Fig. 6. Main defects developing at the aluminum-polymer interface due to (a) insufficient heating and (b) excessive heating conditions (Clamping Frame: Steel).

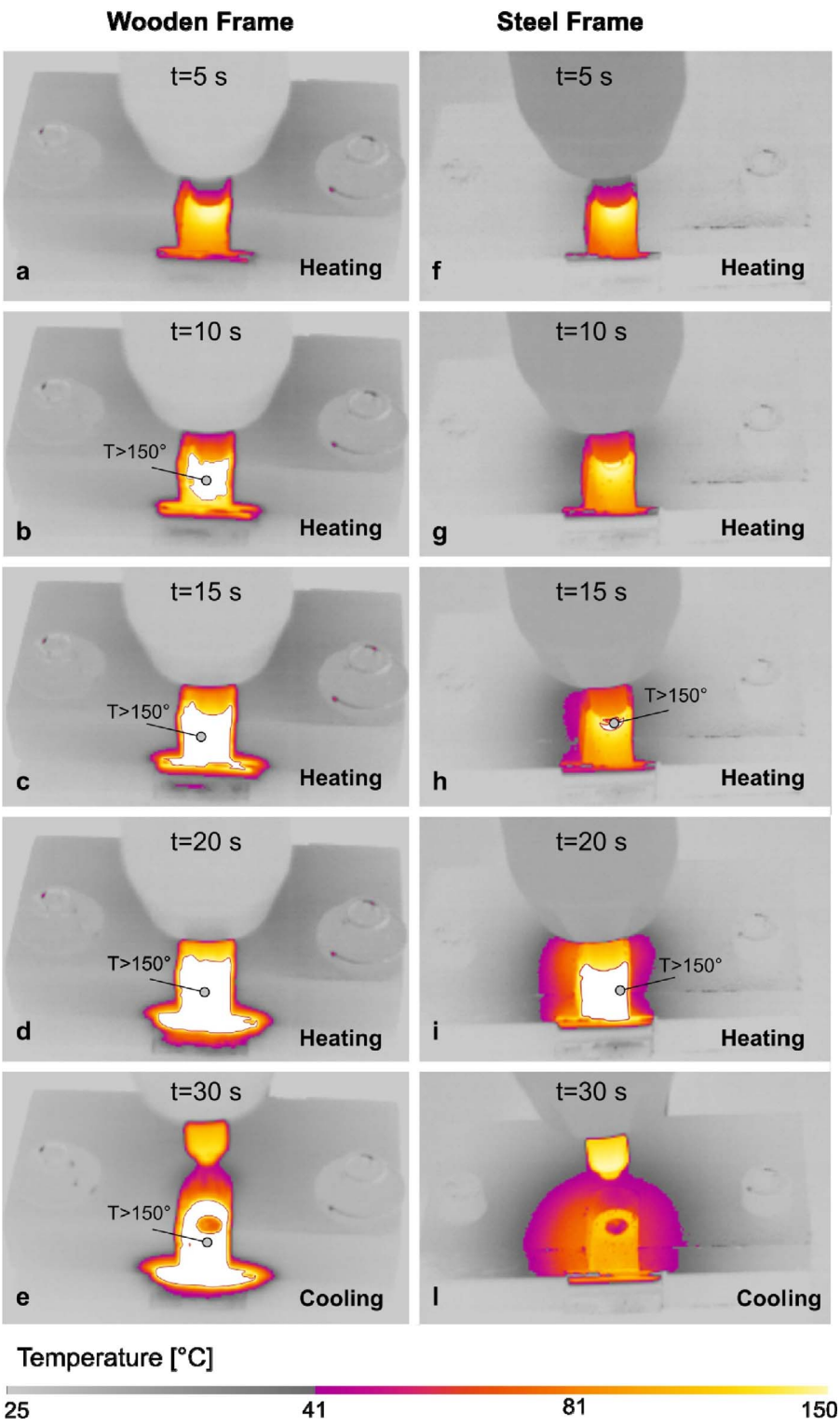

Fig. 7. IR Temperature distribution measured during FSJ with D_t = 20 s, at different processing time (t).

3.2. Thermal analysis

Fig. 7 compares the IR temperature maps performed at different processing times (t) with clamping frames of different materials. As can be observed, until the process time t ≤ 5 s, a negligible difference is observable between the IR maps concerning the different clamping frame materials (Fig. 7a and f). On the other hand, after a longer processing time, the steel frame shows a higher temperature due to its higher thermal conductivity, which indicates a greater energy loss (towards the frame) during the heating phase.

Fig. 8 depicts the variation of the temperature at points P_1 and P_{FRAME} with processing time t. At the beginning of the FAJ process (t < 6 s), the temperature shows a steep increase that is almost identical for the two types of frame. So far, only the material near the tool pin is heated; thus, the heat loss by heat conduction towards the frame is negligible in both cases. The temperature trend shows a knee corresponding to time 6 s and the heating rate reduces. This is due to increasing heat loss by conduction towards the surrounding material and the clamping frame. Thus, after a longer time (t > 6 s), the wooden frame enables higher heating than that achieved by the steel frame

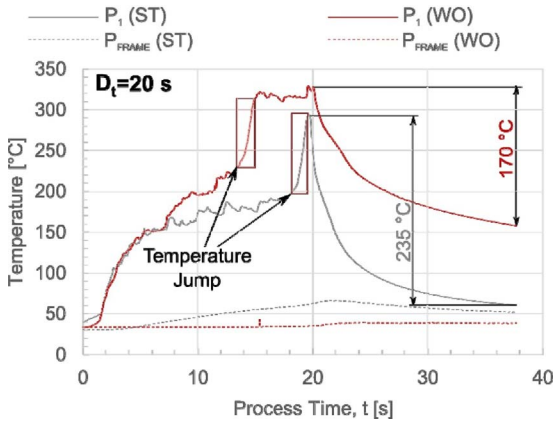

Fig. 8. Temperature variation with processing time at different points: aluminum close to the tool edge (P1) and frame (PFRAME) using wooden and steel frames.

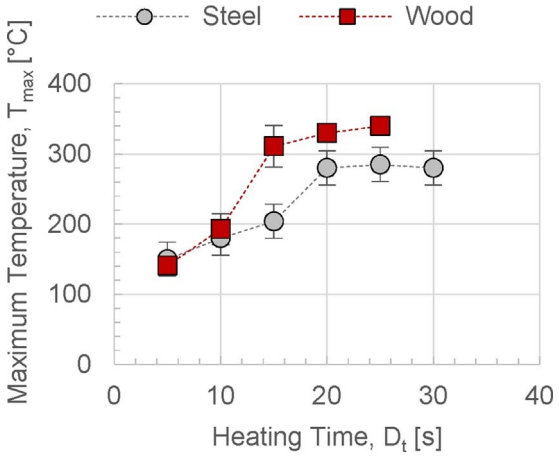

Fig. 10. Variation of maximum temperature reached during FAJ process for different materials of the clamping frame and values of heating time.

because less heat is absorbed by the clamping frame. The temperature of the aluminum surface increases at a constant heating rate until reaching a temperature between 200 and 220 °C. Corresponding to such a temperature, a "temperature jump" was shown, which rapidly raised the temperature to 300–320 °C (in almost two seconds). After reaching that peak, the temperature remained almost constant since the energy absorbed by friction work was almost balanced by the energy loss by heat conduction towards the clamping frame.

Such a "temperature jump" was observed in all the tests performed with the wooden frame with $D_t \geq 15$ s and the steel frame with $D_t \geq 20$ s. This variation was attributed to a significant aluminum surface modification that produced a steep increase in the torque (and thus the energy absorbed) measured during the FAJ process, as reported in Fig. 9a and b.

During the joining process, the top surface of the wooden frame showed a low increase in temperature (less than 10 °C) while that in the steel frame was more significant (up to 36 °C), as can be observed in Fig. 8. This difference is also indicative of the great heat absorbed by the steel frame (with respect to the wooden one) that steals heat to the joint during the heating phase. On the other hand, during the cooling phase, the steel frame enabled faster material cooling due to its higher thermal conductivity. Indeed, after 18 s of cooling (t = 38 s), the temperature at the point P_1 reduced by almost 170 °C with the wooden frame and 235 °C with the steel frame.

Fig. 10 depicts the variation of the maximum temperature T_{max} (temperature at point P_1) produced when varying the clamping frame material and heating time. From Fig. 10, the maximum temperature shows a linear increase with a heating time as long as $T_{max} <$ 200 °C. Then, the temperature increases steeply, due to the aforementioned temperature jump effect. Then, further increase in the heating time resulted in a marginal increase in the temperature since the heat produced by friction is essentially balanced by that lost by conduction towards the clamping frame. It is worth noting that, the adoption of the wooden frame enabled faster heating of the aluminum (and then the materials interface) and produced higher temperatures (T_{max} = 340 °C for D_t = 25 s) as compared to those produced when using the steel frame (T_{max} = 280–300 °C for D_t = 25 s).

The lower conductivity of the wooden frame, which produces a heat-barrier effect, also leads to a lower gradient of temperature along the radial direction (L_1), as can be observed in Fig. 11b. Thus, the wooden frame enables a better homogenization of the temperature over the specimen surface. Besides the higher heating rate, the adoption of a

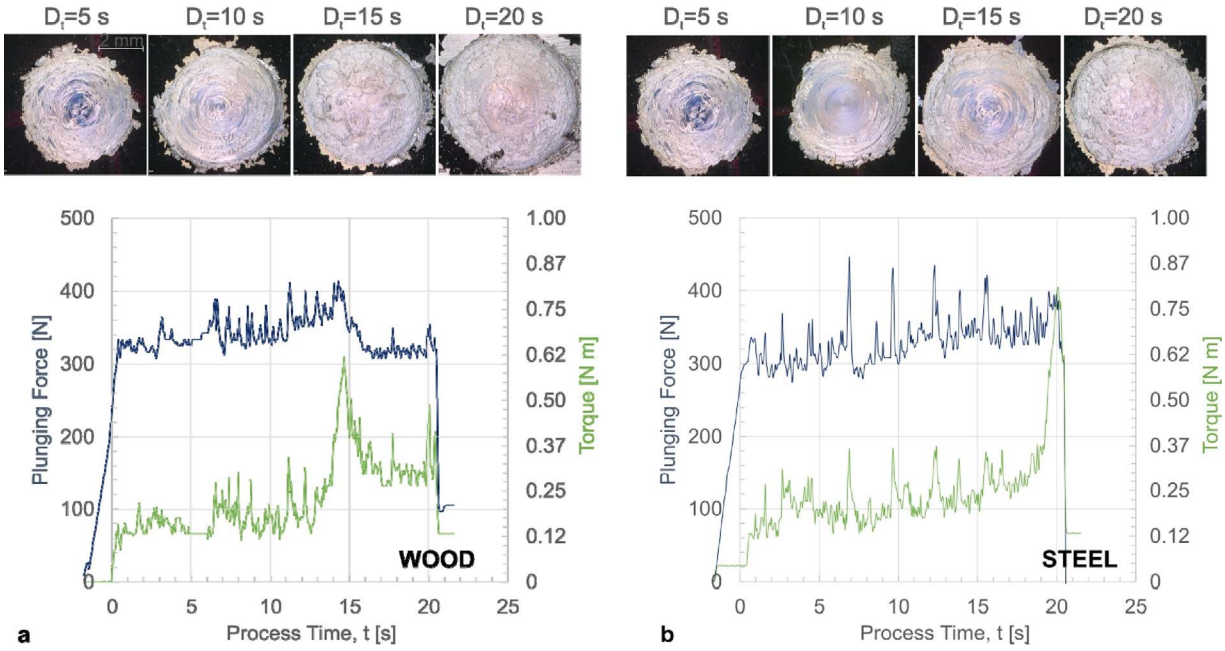

Fig. 9. Variation of Plunging force and torque during FAJ process using (a) wooden frame and (b) steel frame.

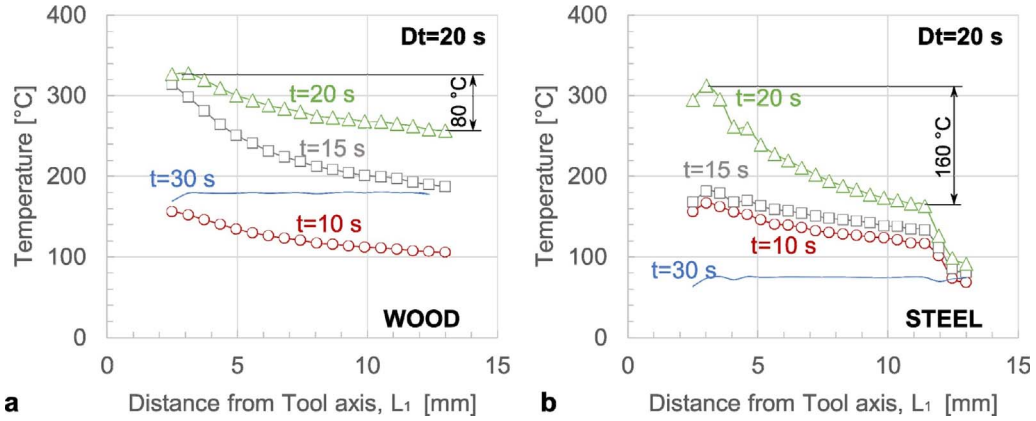

Fig. 11. Temperature distribution along line L_1 after different processing times t and during the cooling phase (t = 30 s) for: (a) wooden frame and (b) steel frame.

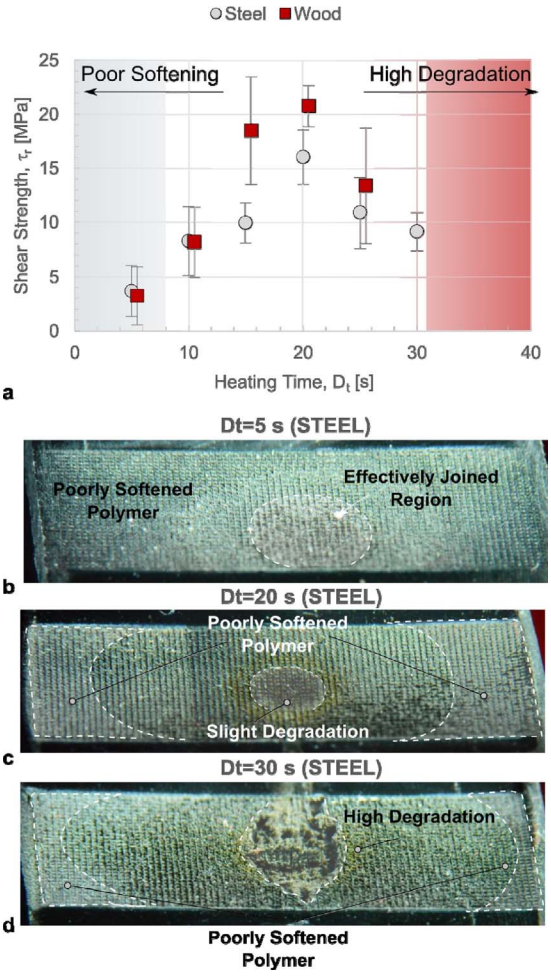

Fig. 12. (a) Variation of the Shear Strength with process parameters and fracture surfaces at different heating times (b) Dt = 5 s, (c) Dt = 20 s and (d) Dt = 30 s.

frame with a lower thermal conductivity (wood) enables greater temperature uniformity between the central and more peripheral region, as depicted in Fig. 11. This becomes particularly evident for a relatively long heating time (t = 20 s) and during the cooling phase (t = 30 s), since the amount of heat loss towards the clamping frame increases with the processing time. Thus, the difference between the temperature gradients become more evident.

3.3. Mechanical behavior of the joints

The variation of the shear strength of the joints τ_r with the heating time D_t and the material of the clamping frame is reported in Fig. 12a. τ_r shows a peak value for D_t = 20 s regardless of the material of the clamping frame. This is due to the presence of different phenomena developing during the FAJ process, namely: poor polymer softening, which is due to the low temperature reached during the heating phase, and polymer degradation (shown in Fig. 14), which is due to excessive heat absorbed during the process, as was also observed by Yusof et al. (2016). Indeed, for short heating times, e.g. D_t = 5 s, a large area of the interface was characterized by poor penetration of the aluminum teeth in the PVC (caused by poor polymer softening), which resulted in weak fastening between the substrates. Thus, the joined region was mainly confined in correspondence of the tool pin, as show in Fig. 12b. Increasing the heating time resulted in a higher temperature at the interface that caused the onset of a negligible degradation in the central region (brown area) but also a larger joined region, as seen in Fig. 12c. However, excessively long heating times resulted in severe degradation of the central region (Fig. 12d).

The employment of the wooden frame enabled joints to be achieved with higher strength τ_{20s} = 20.8 MPa, as compared to those produced by the steel frame τ_{20s} = 16.0 MPa. The wooden frame involved higher temperature in the central region as compared to the steel frame, which caused a higher degradation, as shown in Fig. 12a, Fig. 12c, and Fig. 12e. However, the wooden frame enabled achieving higher temperature in the side region (almost 240 °C) than that produced with the steel frame (140–160 °C). Thus, the wooden frame involved more uniform joining conditions with respect to those achieved by means of the steel frame. This resulted in the achievement of good joining conditions even at the side regions (see Fig. 13d), while unfilled regions were found on the specimens produced by means of the steel frame (Fig. 13b).

Fracture surface analysis was performed to understand the main features of the joints made with different clamping frame materials and D_t = 20 s. Fig. 14 shows the fracture surface of the joint made by the wooden frame. The joint shows a central crater (with a diameter of almost 3 mm) surrounded by a highly degraded region (Fig. 14a). Inside the central crater, the PVC material assumes a closed foam shape characterized by the presence of the aforementioned bubbles (Fig. 14b) due to the high temperature experienced during the heating phase. In correspondence of region 2, the PVC assumes a “lamellae shape”, which is indicative of a greater material degradation (Fig. 14c). This is due to the higher temperature experienced in correspondence of the tool edge (due to higher tangential velocity). This effect is even more marked inside the region 3, where severe PVC degradation is shown (Fig. 14d). The strength in correspondence of these three regions is very poor, since the reduction of the resisting area and high stress concentration. On the other hand, the degraded region is surrounded by large areas where the PVC was tightly fastened to the aluminum teeth, as shown in Fig. 14e-g, which provided the main contribute to the joint strength. These areas were observable even in correspondence of the side region.

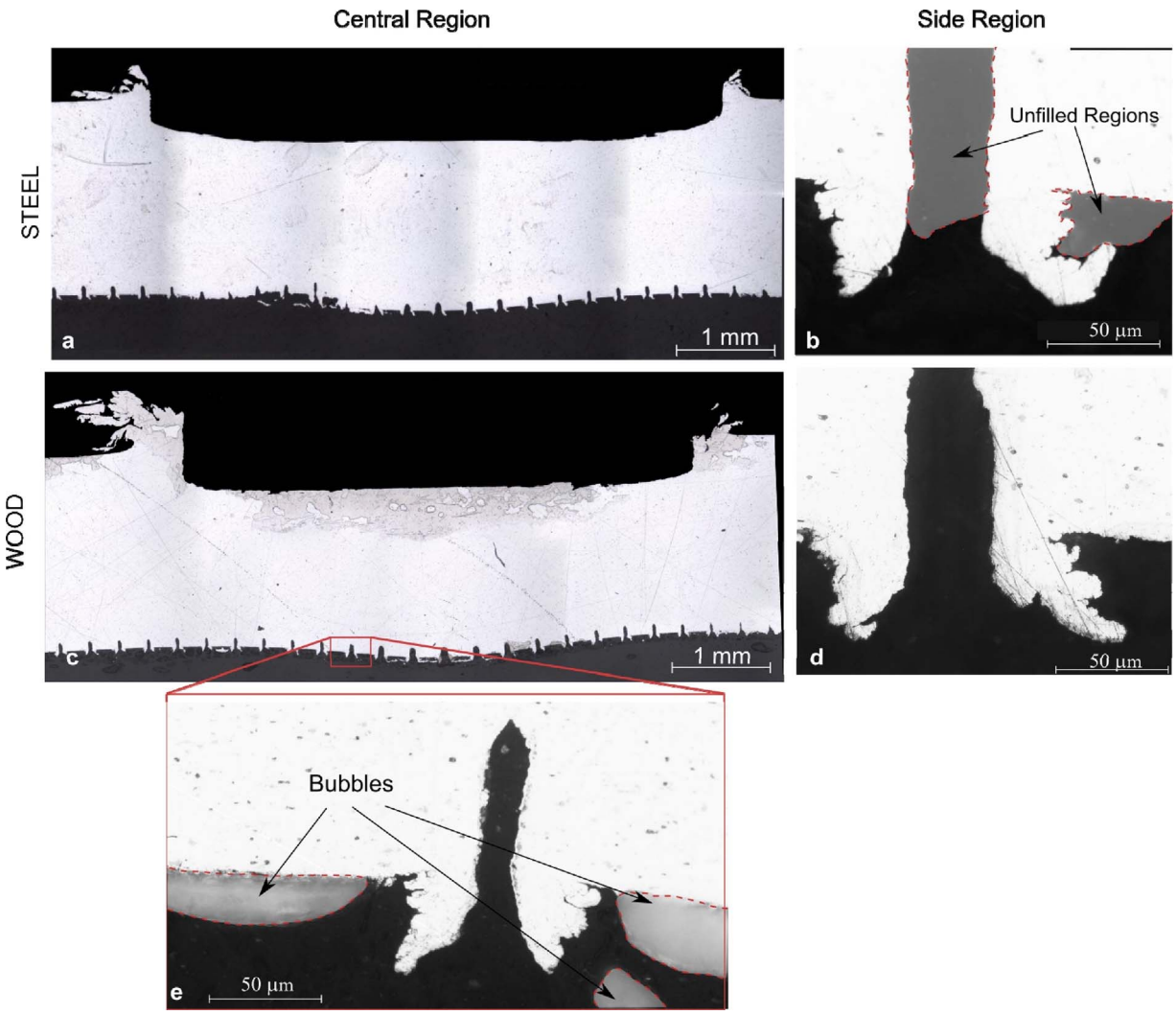

Fig. 13. Cross sections of the specimens produced with steel and wood frames, in the central and side regions (D_t = 20 s).

The fracture surface on specimens joined with the steel frame showed different features. Actually, in the central region the PVC did not show the onset of degradation and it appeared tightly fastened to the aluminum teeth (Fig. 15a and Fig. 15b). This was due to the great polymer softening given the high temperature, which enabled a deep penetration of the aluminum teeth inside the polymer. On the other hand, small areas of the polymer remained attached to the aluminum substrate since the low temperature experienced during the joining process (T_{max} < 200 °C). These regions, reported in Fig. 15d, provided a lower strength as compared to the corresponding areas on specimens made with the wooden frame, shown in Fig. 14g and Fig. 14f.

Fig. 16 shows the fracture surface on the PVC substrate (Dt = 20 s) made with both the clamping frames. The comparison of Fig. 16a and c confirms the higher degradation achieved in the central zone when the wood frame is adopted, while in the case of the steel frame the degradation temperature of the PVC (293 °C) is only approached. When the steel frame was used, the fracture surface in the side region showed shallow imprints made by the aluminum teeth, which indicate poor penetration of the aluminum within the polymer (Fig. 16b). On the other hand, when the wooden frame was used, the aluminum teeth produced deeper groves on the polymer surface since the greater softening due to the higher temperature (Fig. 16d). These regions increased the strength of these joints, which were characterized by a higher average strength as compared to that produced by using the steel frame.

Considering the equivalent von Mises shear strength of the PVC material $\tau_{max} = B\sigma_{max}/\sqrt{3}$ = 21.4 MPa, under the optimal processing conditions, the joint efficiency (calculated as the ratio of the shear strength to that of the base material) reached almost 97.2%. This means that the strength of the joint is very close to that of the material with the weaker strength.

Besides the advantages in terms of higher joints strength, from a process point of view, the energy absorption is also a major concern. Fig. 17(a) depicts the energy calculated by means of Eq. (1) for the analyzed cases. It is evident that the energy absorbed increases almost linearly with the heating time (with the exception of a small steep increase corresponding to the “temperature jump” conditions), while the material of the clamping frame has a negligible influence on the absorbed energy. Thus, considering the trend of the shear strength of the joints vs. the absorbed energy, as reported in Fig. 17(b) it is found that the wooden frame involves higher energy efficiency since more energy is stored in the joint during the heating phase as well as the more uniform temperature distribution produced.

4. Conclusions

The main achievements of the present study are summarized as follows:

- the proposed clamping frame with low thermal conductivity (made of wood material) has been successfully demonstrated to increase

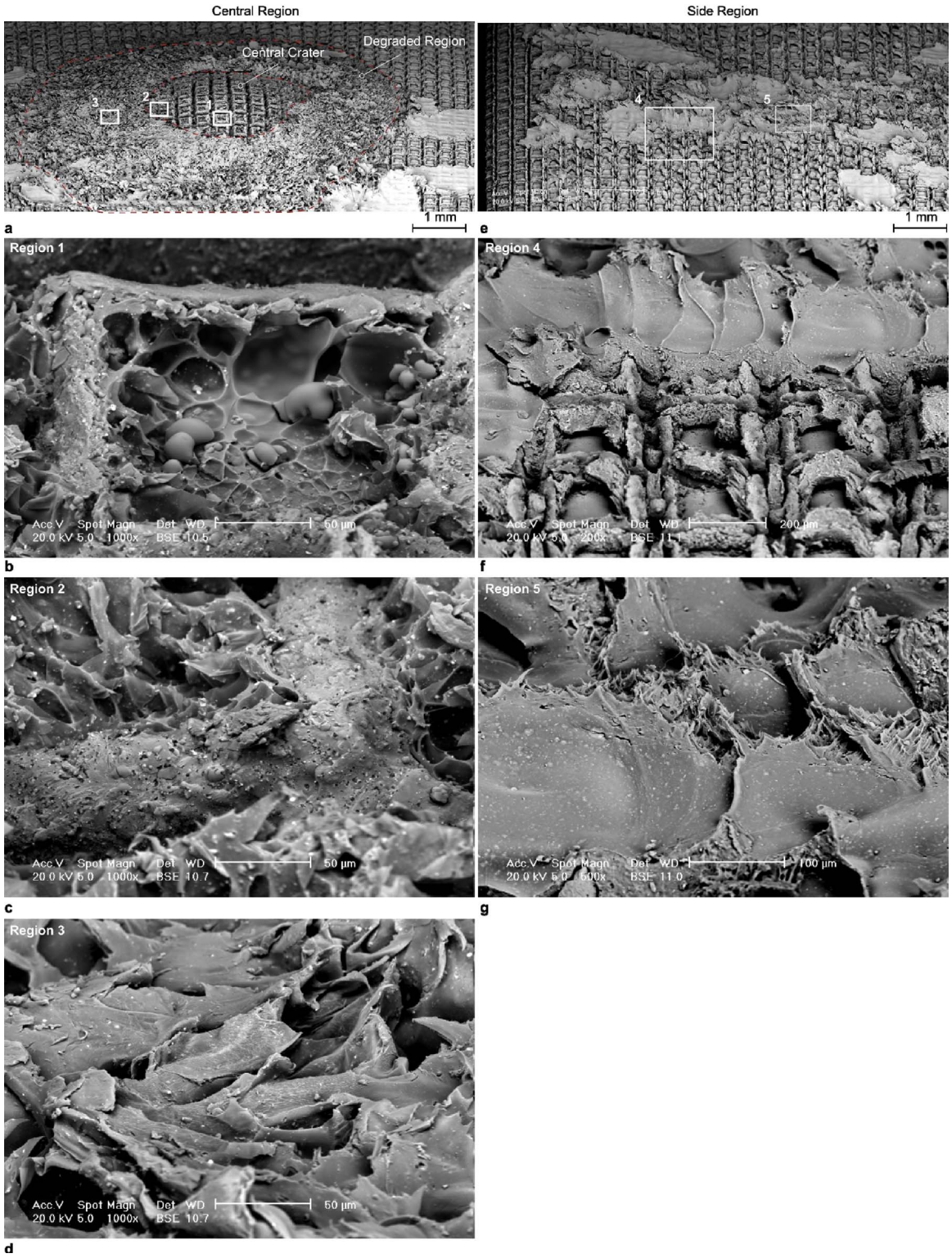

Fig. 14. SEM micrographs of fracture surface on aluminum substrate (D_t = 20 s, clamping frame: wood).

the joints strength made by Friction Assisted Joining with an increase in the efficiency of the energy absorbed during the joining process.

- the adoption of the wooden frame involved temperature gradients between the center of the joint and the periphery. Under optimal conditions, the temperature variation between the center and the periphery were almost 80 °C and 160 °C for the wooden frame and steel frame, respectively.
- the reduction in the temperature gradients produced joints with higher strength since a greater portion of the joined area experienced similar (optimal) joining conditions. Indeed, the highest strength of the joints made with the wooden frame was 20.5 MPa (joint efficiency of 97.2%), while that of the joints made with the steel frame was almost 16 MPa.
- the optimal conditions, which enabled the strength of the joints to be maximized involved a heating time D_t of 20 s regardless of the

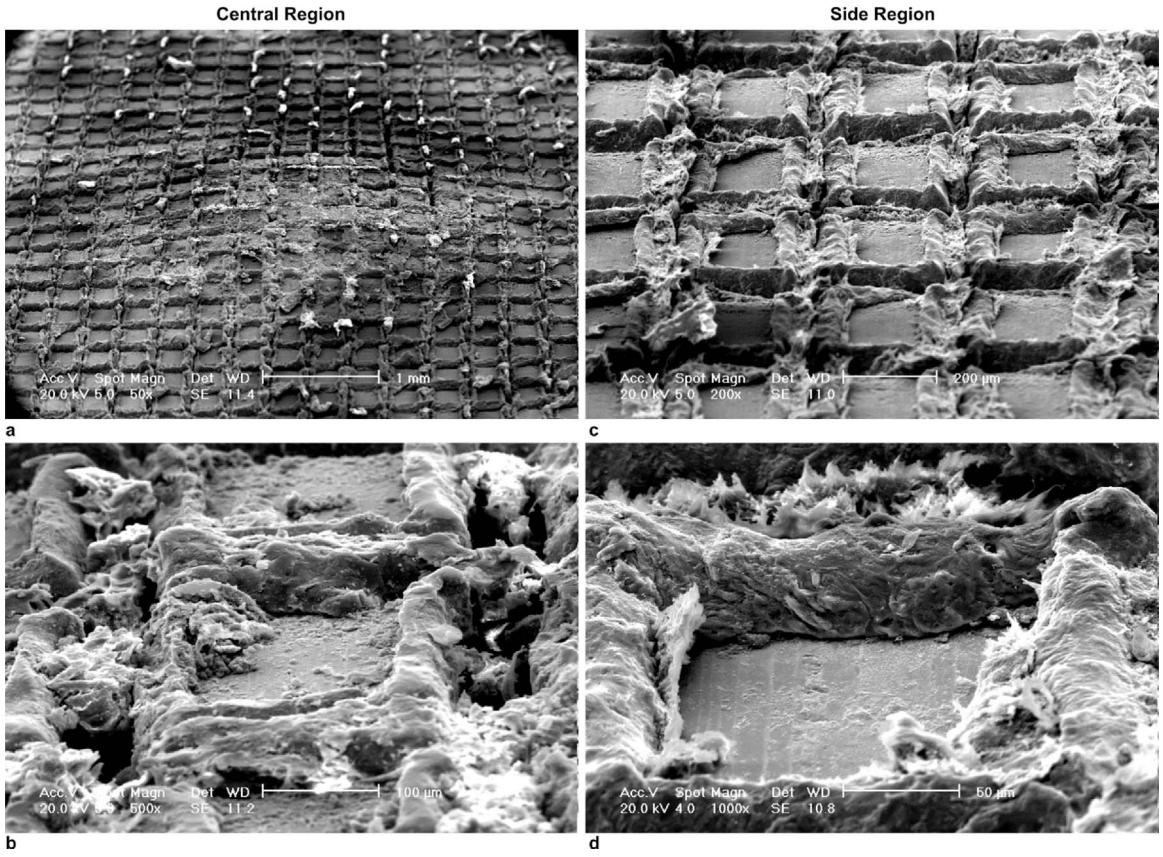

Fig. 15. SEM micrographs of fracture surface on aluminum substrate (D_t = 20 s, clamping frame: steel).

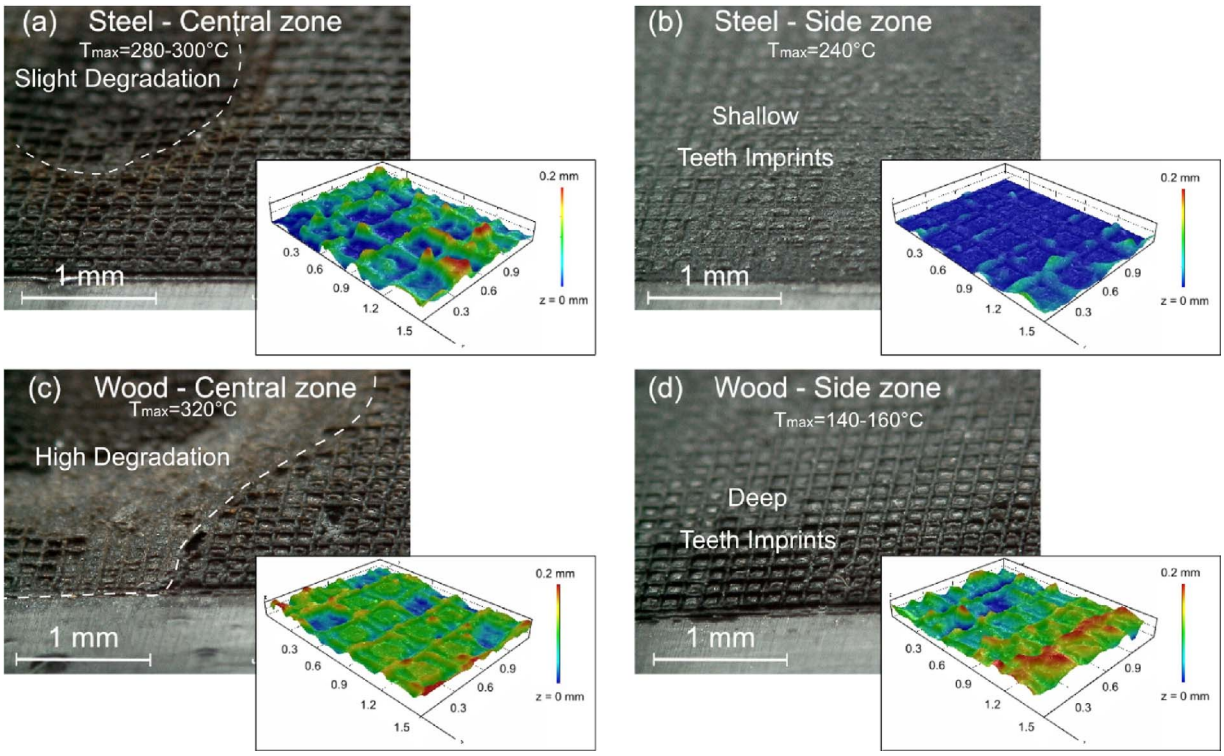

Fig. 16. Fracture surface analysis of the joints (PVC side) performed under optimal conditions (D_t = 20 s) and different clamping frame materials (T_{max} – maximum temperature reached during heating phase).

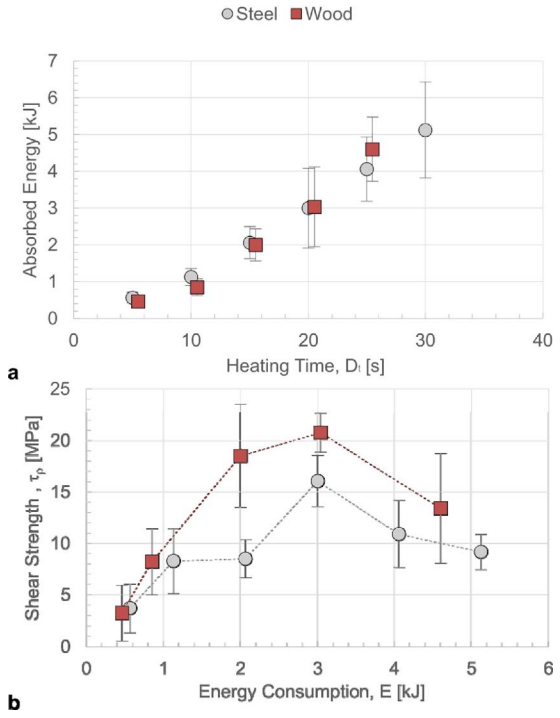

Fig. 17. (a) Variation of the absorbed energy with processing parameters and (b) variation of the Shear Strength with absorbed energy.

material of the frame. The adoption of the wooden frame could also be exploited to achieve the same strength as the joints made by the steel frame but within a lower processing time.

- the maximum strength (16 MPa) of the joints made by the steel frame was produced after a heating time of 20 s. A higher value of strength (18.5 MPa) could be achieved by using the wooden frame with a lower heating time (D_t = 15 s). This also comes with a reduction in the absorbed energy: almost 3 kJ and 2.0 kJ for the steel and wooden frame, respectively.

Acknowledgements

The authors wish to thank Mr. Giuseppe Organtini (DIIIE, University of l'Aquila) for his contribution during the setup and performance of the experimental tests. The authors wish also to thank Mrs. Fabiola Ferrante (DIIIE, University of l'Aquila) for her contribute during TGA tests. Finally, the authors are grateful to doc and doc. Lorenzo Arrizza (microscopy center of University of l'Aquila) for SEM analysis of fracture surfaces.

References

ASTM D 638, 2000a. Standard Test Method for Tensile Properties of Plastics.
ASTM E 8 M, 2000b. Standard Test Methods for Tension Testing of Metallic Materials [Metric].
Abibe, A.B., Sônego, M., dos Santos, J.F., Canto, L.B., Amancio-Filho, S.T., 2016. On the feasibility of a friction-based staking joining method for polymer-metal hybrid structures. Mater. Design 92, 632–642.
Di Franco, G., Fratini, L., Pasta, A., 2012. Influence of the distance between rivets in self-piercing riveting bonded joints made of carbon fiber panels and AA2024 blanks. Mater. Design 35, 342–349.
Goushegir, S.M., dos Santos, J.F., Amancio-Filho, S.T., 2014. Friction Spot Joining of aluminum AA2024/carbon-fiber reinforced poly(phenylene sulfide) composite single lap joints: microstructure and mechanical performance. Mater. Design 54, 196–206.
Goushegir, S.M., dos Santos, J.F., Amancio-Filho, S.T., 2015. Influence of process parameters on mechanical performance and bonding area of AA2024/carbon-fiber-reinforced poly(phenylene sulfide) friction spot single lap joints. Mater. Design 83, 431–442.
Katayama, S., Kawahito, Y., 2008. Laser direct joining of metal and plastic. Scr. Mater. 59, 1247–1250.
Khodabakhshi, F., Haghshenas, M.-, Chen, J., Shalchi Amirkhiz, B., Li, J., Gerlich, A.P., 2017. Bonding mechanism and interface characterisation during dissimilar friction stir welding of an aluminium/polymer bi-material joint. Sci. Technol. Weld. Join. 22, 182–190.
Lambiase, F., Durante, M., 2017. Mechanical behavior of punched holes produced on thin glass fiber reinforced plastic laminates. Compos. Struct. 173, 25–34.
Lambiase, F., Genna, S., 2017. Laser-assisted direct joining of AISI304 stainless steel with polycarbonate sheets: thermal analysis, mechanical characterization, and bonds morphology. Optics Laser Technol. 88, 205–214.
Lambiase, F., Ko, D.-C., 2016. Feasibility of mechanical clinching for joining aluminum AA6082-T6 and Carbon Fiber Reinforced Polymer sheets. Mater. Design 107, 341–352.
Lambiase, F., Ko, D.-C., 2017. Two-steps clinching of aluminum and carbon fiber reinforced polymer sheets. Compos. Struct. 164, 180–188.
Lambiase, F., Genna, S., Leone, C., Paoletti, A., 2017. Laser-assisted direct-joining of carbon fibre reinforced plastic with thermosetting matrix to polycarbonate sheets. Optics Laser Technol. 94, 45–58.
Lee, C.-J., Lee, J.-M., Ryu, H.-Y., Lee, K.-H., Kim, B.-M., Ko, D.-C., 2014. Design of hole-clinching process for joining of dissimilar materials − Al6061-T4 alloy with DP780 steel, hot-pressed 22MnB5 steel, and carbon fiber reinforced plastic. J. Mater. Process. Technol. 214, 2169–2178.
Liu, F.C., Liao, J., Nakata, K., 2014. Joining of metal to plastic using friction lap welding. Mater. Design 54, 236–244.
Matweb - American Black Walnut Wood.
Nagatsuka, K., Yoshida, S., Tsuchiya, A., Nakata, K., 2015. Direct joining of carbon-fiber-reinforced plastic to an aluminum alloy using friction lap joining. Compos. Part B-Eng. 73, 82–88.
Okada, T., Uchida, S., Nakata, K., 2014. Direct joining of aluminum alloy and plastic sheets by friction lap processing. Mater. Sci. Forum 794 (-796), 395–400.
Pardal, G., Meco, S., Dunn, A., Williams, S., Ganguly, S., Hand, D.P., Wlodarczyk, K.L., 2017. Laser spot welding of laser textured steel to aluminium. J. Mater. Process. Technol. 241, 24–35.
Rodríguez-Vidal, E., Sanz, C., Soriano, C., Leunda, J., Verhaeghe, G., 2016. Effect of metal micro-structuring on the mechanical behavior of polymer-metal laser T-joints. J. Mater. Process. Technol. 229, 668–677.
Yu, J., Sun, L., Ma, C., Qiao, Y., Yao, H., 2016. Thermal degradation of PVC. A Rev. Waste Manage. 48, 300–314.
Yusof, F., Yukio, M., Yoshiharu, M., Abdul Shukor, M.H., 2012. Effect of anodizing on pulsed Nd:YAG laser joining of polyethylene terephthalate (PET) and aluminium alloy (A5052). Mater. Design 37, 410–415.
Yusof, F., Muhamad, M., Moshwan, R., Jamaludin, M., Miyashita, Y., 2016. Effect of surface states on joining mechanisms and mechanical properties of aluminum alloy (A5052) and polyethylene terephthalate (PET) by dissimilar friction spot welding. Metals 6, 101.
Zhang, Z., Shan, J., Tan, X., Zhang, J., 2016. Improvement of the Laser Joining of CFRP and Aluminum via Laser Pre-treatment The International Journal of Advanced Manufacturing Technology.